

Shear Viscosity, Extensional Viscosity, and Die Swell of Polypropylene in Capillary Flow with Pressure Dependency

JAN-CHAN HUANG, KIM-SWEET LEONG

Plastics Engineering Department, University of Massachusetts at Lowell, Lowell, Massachusetts 01854

Received 20 April 2001; accepted 15 September 2001

ABSTRACT: The shear and extensional viscosities of a polypropylene resin were studied using a capillary rheometer and capillary dies of 1-mm diameter and length of 10, 20, and 30 mm. Melt temperatures at 190, 205, and 220°C and shear rates between 100 and 5000 s⁻¹ were used. At the highest shear rate a visible melt fracture was observed. An equation relating the pressure drop and die length was derived with consideration of pressure effects on melt viscosities and the end effect. After the correction for pressure effects the true wall shear stress and end effect at zero pressure were calculated. The end effect showed a critical stress of melt fracture around 10⁵ Pa, and increased rapidly when shear stress increased above the critical stress. From shear stress the shear viscosity was calculated, and a power law behavior was observed. Extensional viscosity was calculated from the end effect and showed a decreasing trend when strain rate increased. After time–temperature superposition shift shear viscosity data correlated well, but an upward trend was observed in extensional viscosity when melt fracture occurred. Die swell ratio at different temperatures can be plotted as a function of wall shear stress and was higher for shorter dies. © 2002 Wiley Periodicals, Inc. *J Appl Polym Sci* 84: 1269–1276, 2002; DOI 10.1002/app.10466

Key words: poly(propylene); viscosity; rheology; melt fracture

INTRODUCTION

The flow behavior of polymer melts is of great practical importance in the design of polymer-processing equipment. Knowledge of rheological characteristics helps one to choose the right processing conditions. The upper limit of processing rate of a polymer is mainly controlled by its melt viscosity and the occurrence of the melt fracture phenomena. Shear viscosity determines the level of power requirement for processing equipment. The shear rate dependency of shear viscosity determines the sensitivity of the power requirement

with respect to a change of processing speed. For a polymer with Newtonian viscosity the power requirement is proportional to the square of processing speed, while for a non-Newtonian fluid the dependency is less. The operating range of a non-Newtonian fluid is wider than a Newtonian fluid. Extensional viscosity is another important rheological property in processes such as fiber spinning, film blowing, and blow molding. Studies of extensional viscosity of polymer melts are not as comprehensive as studies of shear viscosity. Melt fracture is a flow instability phenomenon that may limit production rates in polymer processing. The term “melt fracture” is used to describe extrudate distortion or variation of the shape of extrudates. These distortions appear when shear stresses of a polymer melt exceed a critical value.^{1–3}

Correspondence to: J.-C. Huang (Jan_Huang@uml.edu).

Journal of Applied Polymer Science, Vol. 84, 1269–1276 (2002)
© 2002 Wiley Periodicals, Inc.

The capillary rheometer is widely used to measure shear viscosity and extensional viscosity, and to observe the melt fracture of polymer melts. A careful measurement of viscosity requires at least two different die lengths running at the same flow rate to calculate the end correction.^{4,5} If the melt viscosity and the end correction at the die entrance are pressure independent, the pressure drop across the capillary, ΔP , is related to capillary length, L , by:

$$\Delta P = 2\tau_w(L/R + e) \quad (1)$$

From this plot the wall shear stress, τ_w , and the end effect, e , can be determined. This is the Bagley plot.^{4,5} Equation (1) is commonly used in the capillary rheometer study when the pressure effect on melt properties is not significant and the plot is linear. The calculation of shear viscosity starts from the apparent shear rate, $\dot{\gamma}_a$, which is related to the volume flow rate, Q , by:

$$\dot{\gamma}_a = 4Q/\pi R^3 \quad (2)$$

The apparent shear rate is an average calculated based on the Newtonian fluid assumption. A Rabinowitsch correction is required to correct the non-Newtonian effect.^{4,6} The slope of a double logarithmic plot τ_w vs. $\dot{\gamma}_a$ gives the slope, n . From the power law index the shear rate, $\dot{\gamma}$, is calculated from the following equation:

$$\dot{\gamma} = \dot{\gamma}_a(3n + 1)/4n \quad (3)$$

with the shear rate, $\dot{\gamma}$, the viscosity, η , is calculated as:

$$\eta = \tau_w/\dot{\gamma} \quad (4)$$

From the end effect extensional viscosity, η_e , as the function of extensional rate, $\dot{\epsilon}$, can be calculated based on equations derived by Cogswell:⁷

$$\eta_e(\dot{\epsilon}) = \frac{9(n + 1)^2}{32\tau_w} \frac{\Delta P_{\text{ent}}^2}{\dot{\gamma}_a} \quad (5)$$

$$\dot{\epsilon} = \frac{4\tau_w\dot{\gamma}_a}{3(n + 1)\Delta P_{\text{ent}}} \quad (6)$$

where n is the slope used in eq. (3) and ΔP_{ent} is the entrance pressure drop corresponding to zero capillary length. In the derivation of eqs. (5) and

(6) it was assumed that the polymer melt adopted a conical-cylindrical flow pattern as it flowed from the barrel into the capillary die. It was also assumed that the shear viscosity of the polymer melt can be described by a power-law model. These equations were used to determine the extensional viscosity of polypropylene by Hingman et al.⁸ and Tzoganakis et al.⁹ Because of the relationship in eq. (6) the strain rate range of extensional viscosity measured through the end effect is about 10 times lower than the corresponding range of shear rate.

PRESSURE EFFECTS IN CAPILLARY FLOW

When high shear rate and long capillaries were used, upward deviations were observed in comparison with short capillaries at the same shear rate.⁹⁻¹³ This was explained by the pressure dependence of the shear viscosity. The following expression has been used to describe the effect of pressure on shear viscosity:⁹⁻¹⁴

$$\eta = \eta_o e^{\beta P} \quad (7)$$

where η_o is the shear viscosity at zero pressure, and β is the pressure coefficient. Because the viscosity of polymer melts increases as pressure increases, the rate of pressure drop varies throughout capillary length and a nonlinear pressure vs. length curve was observed. To derive the mathematical relationship we take the momentum balance over an infinitely small length of the capillary die to give:

$$\pi R^2 dP = 2\pi R \tau_w dz \quad (8)$$

Note that

$$\tau_w = \eta \dot{\gamma} = \eta_o e^{\beta P} \dot{\gamma} = e^{\beta P} \tau_{tw} \quad (9)$$

Here, τ_{tw} is the true wall shear stress calculated using shear viscosity at zero pressure. Substitution of eq. (9) into eq. (8) gives

$$e^{-\beta P} dP = 2 \left(\frac{dz}{R} \right) \tau_{tw} \quad (10)$$

Integration of eq. (10) over capillary length gives:

$$(1 - e^{-\beta P})/\beta = (2L/R)\tau_{tw} \quad (11)$$

Here we assume the hydrostatic pressure is zero at the capillary outlet ($L = 0$). If we add the end correction, eq. (11) becomes:^{11,12}

$$(1 - e^{-\beta P})/\beta = 2\tau_{tw}(L/R + e) \quad (12)$$

When β is small, eq. (12) becomes eq. (1), and the true wall shear stress becomes τ_w . Recently, Bindings et al.¹⁴ determined the pressure dependency of shear viscosity and extensional viscosity of several polymers using a capillary rheometer that could be pressurized at both entrance and outlet. The pressure drop was kept small while overall pressure was varied from zero to 70 MPa. It turned out that the pressure dependency of extensional viscosity was higher than shear viscosity for polypropylene, polystyrene, and poly methyl(methacrylate). For low density polyethylene the values were similar. Because the end effect is a function of extensional viscosity, the pressure dependency will give the same dependency on the end effect. In light of this observation, eq. (12) should be modified to include a separate dependency of the end effect. The end effect is separated into a product of the zero pressure component " E " and its pressure dependency: $e = E e^{\alpha P}$. The parameter α is the pressure dependency coefficient of extensional viscosity, and P is the barrel pressure where the end effect took place. The final result is:

$$(1 - e^{-\beta P})/\beta = 2\tau_{tw}[(L/R) + E e^{\alpha P}] \quad (13)$$

or

$$(1 - e^{-\beta P})e^{-\alpha P}/\beta = 2\tau_{tw}[(L/R)e^{-\alpha P} + E] \quad (14)$$

If parameters α and β are known, the left-hand side of eq. (14) can yield a linear plot vs. $(L/R)e^{-\alpha P}$. Equation (14) contains four unknown parameters compared to two parameters in the Bagley equation. The determination of both α and β , using pressure drop from different die length, cannot produce reliable results because both of them have similar effects on the curvature of the pressure vs. length plot. A separate knowledge of α and β is necessary to calculate wall shear stress and the end effect. In this study we used the pressure dependency data in the literature to verify the use of eq. (14).

EXPERIMENTAL

The material used in this study was Atofina 3622 polypropylene resin manufactured by Atofina. It

is an injection-molding grade homopolymer with number-average molecular weight 29,000 and weight-average molecular weight 190,000. The melt flow index measured by ASTM D1238 condition L is 12 g/10 min. The information was provided by the manufacturer. The rheological properties were measured by a Ceast Rheovis 2100 capillary rheometer. The rheometer was equipped with a computer for data acquisition. The pressure sensors of the capillary rheometer was located at the capillary entrance. Three carbide capillaries with flat entrance region were used. The diameter was 1 mm, and the die lengths were 10, 20, and 30 mm. These gave L/R ratio of 20, 40, and 60, respectively. Six different shear rates from 100 s^{-1} to 5000 s^{-1} were used. Three temperatures, 190, 205, and 220°C , were chosen for this study. Extrudates were collected to observe melt fracture and measure die swell.

RESULTS AND DISCUSSION

One method to estimate the critical shear stress is to observe the extrudate from the capillary die. When the shear stress exceeds the critical stress the extrudate tends to experience melt fracture phenomena. Figure 1 shows the extrudates at 190°C for the 20-mm die. It can be seen that a periodic pattern appeared on extrudates when the apparent shear rates was 5000 s^{-1} . Only the highest shear rate produced a visible melt fracture. The critical stress was likely to occur between shear rates 2000 and 5000 s^{-1} .

To verify any pressure effect the pressure drop readings were plotted vs. L/R for each shear rate. Figure 2 shows the pressure vs. L/R for 190°C . It can be seen that an upward trend existed for each shear rate. A pressure correction was needed. In a previous report¹¹ the value of β of a polypropylene resin was determined to be 18 GPa^{-1} at 190°C using eq. (12). Because the extensional viscosity increased when barrel pressure increased, the end effect also increased. This gave a higher end effect for a longer capillary and the value of β determined from eq. (12) tends to be overstated. In a study of polypropylene made by Kazatchkov et al.¹³ the entrance effect was measured by dies with zero length and the pressure coefficient of shear viscosity was determined by the superposition of shear stress vs. apparent shear rate data into a master curve. The best value for their data was estimated to be in the range of $5.9\text{--}10 \text{ GPa}^{-1}$. Binding et al.¹⁴ determined the pressure depen-

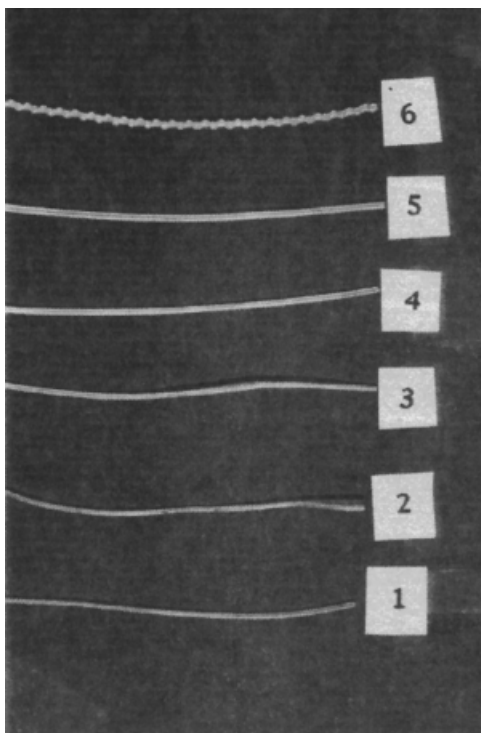


Figure 1 Extrudates of Atofina 3622 polypropylene at 190°C and die length = 20 mm. From top to bottom the apparent shear rates are 5000, 2000, 1000, 500, 200, and 100, respectively.

dency of shear viscosity and end effect by using a capillary rheometer equipped with a second chamber, which could increase the end pressure of a capillary die. Using their data the values of β

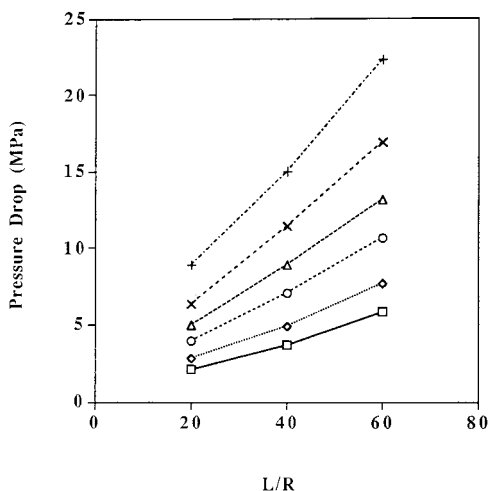


Figure 2 Pressure drop of capillary die vs. L/R at 190°C. From top to bottom the apparent shear rates are 5000, 2000, 1000, 500, 200, and 100, respectively.

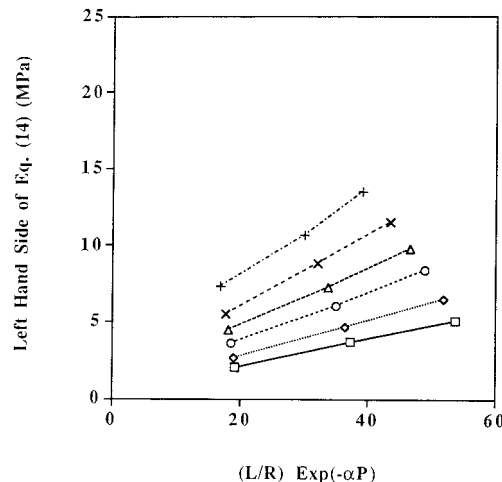


Figure 3 The left-hand side of eq. (14) vs. $(L/R)\text{Exp}(-\alpha P)$ at 190°C. From top to bottom the apparent shear rates are 5000, 2000, 1000, 500, 200, and 100, respectively.

were estimated to be 7.1, 7.0, and 6.8 GPa^{-1} for 190, 205, and 220°C, respectively. The values of α were 19.1, 17.7, and 16.4 GPa^{-1} for 190, 205, and 220°C, respectively. These figures were used in our calculation.

Figure 3 shows the left-hand side of eq. (14) vs. $(L/R)\text{Exp}(-\alpha P)$ for the same apparent shear rates as Figure 2. Straighter lines were observed in Figure 3. The highest shear rate still showed some upward curvature. This was because the highest shear rate had the melt fracture phenomenon, which could affect the results. It was noted that the horizontal variables on Figure 3 were no longer on a constant interval. The values of higher shear rate decreased because they were multiplied by a smaller value of $\text{Exp}(-\alpha P)$. Parameter β also decreased the value of the left-hand side of Eq. (14). Therefore, the inclusion of both α and β reduced the left-hand side. This mathematical effect made the experimental determination of the two parameters, α and β , using eq. (14) difficult. In this study we chose to use the results in the literature so that α and β were no longer adjustable parameters. True wall shear stress, τ_{tw} , and the end effect at the zero pressure, E , were calculated from the slope and intercept of these lines using the linear least-square methods.

Temperature increase due to viscous heating could also cause a nonlinear relationship in the pressure vs. length plot. The effect of viscous heating can be estimated from adiabatic heating based on the first law of thermodynamics:

$$\Delta T = \Delta P / \rho C_p \tag{15}$$

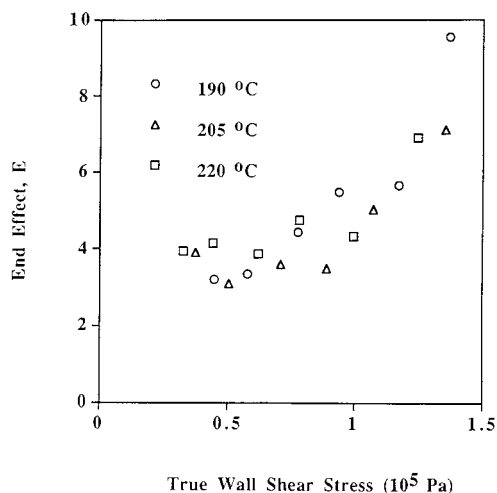


Figure 4 End correction at zero pressure vs. true wall shear stress of polypropylene. Symbols: (○) 190°C; (△) 205°C; (□) 220°C.

where ρ is the density and C_p is the specific heat of polypropylene. In an adiabatic process all pressure energy is converted into thermal energy. The largest temperature increase occurred at the lowest barrel temperature and highest shear rate. This was because the melt viscosity and barrel pressure were the highest at this condition. Using the density value of 850 kg/m³ and specific heat of 2700 kJ/kg °C for polypropylene the maximum temperature increase was estimated to be 9.7°C. Note that this number was reduced by heat conduction through the die surface. The temperature increase tended to lower the pressure reading at the higher pressure. The effect was to reduce the curvature of the pressure-length curve, and could mask some of the pressure effect on shear viscosity. For this reason the differential method used by Binding et al.¹⁴ would be better for the determination of parameters.

The end effect at zero pressure, E , was plotted vs. true wall shear stress, τ_{tw} , in Figure 4. Results of the three temperatures were plotted on the same figure. It can be seen that data for the three temperatures followed the same trend. At stress below 10⁵ Pa the end effect increased slowly when stress increased. Above this critical stress the rate of increase was much higher. The effect of temperature was small because data could be plot as a master curve of shear stress. Vlachopoulos and Alam¹⁵ showed that for polyethylene the ratio of critical stress and absolute temperature was a function of molecular weights. This gave a small temperature dependency for critical shear stress.

The value of critical stress in this study was close to our previous study on another grade of polypropylene.¹¹ Kazatchkov et al.¹³ also reported the occurrence of melt fracture of polypropylene in the range of 0.12 to 0.15 MPa. Ui et al.¹⁶ found the melt fracture for a series of polypropylenes to be in the range between 0.1 and 0.13 MPa. More recently, Baik and Tzoganakis¹⁷ measured the extrudate distortion of a series of polypropylenes prepared by peroxide degradation. The critical shear stress was found to decrease linearly from 0.15 to 0.10 MPa when the weight-average molecular weight increased from 100,000 to 400,000. The result of this study was at the lower end of the literature results. This was due to the correction of the pressure effect in this study. After removal of the pressure effect the true wall shear stress was lower than the corresponding stress without correction, τ_w .

The calculation of shear viscosity started from a plot of true wall shear stress vs. the apparent shear rate on a double logarithm scale. The slope of this plot gave the slope n . These results were used to calculate shear viscosity based on the Rabinowitsh correction described in eqs. (3) and (4). For most unfilled polymers the shear viscosity at different temperatures can be shifted into a master curve by time-temperature superposition. Figure 5 shows the melt viscosity of polypropylene after high temperature data were shifted to 190°C. The shift was made based on the following formula:¹⁸

$$\eta(\dot{\gamma}/a_T) = \eta(\dot{\gamma})T_0/a_T T \quad (16)$$

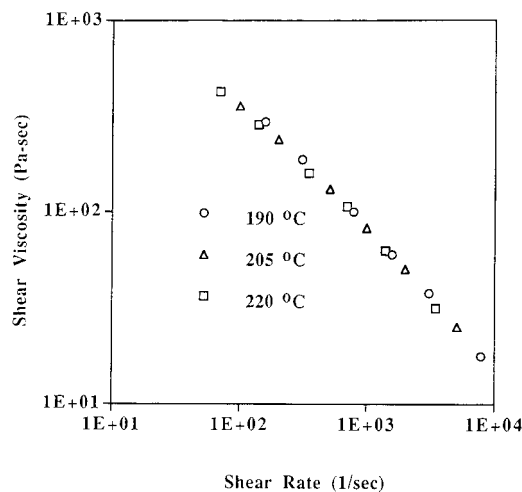


Figure 5 Shear viscosity vs. true wall shear rate of polypropylene. High temperature data were shifted to 190°C. Symbols: (○) 190°C; (△) 205°C; (□) 220°C.

The shift factors were 1.5 and 2.1 for 205 and 220°C, respectively. The results of shear viscosity in Figure 6 showed a strong shear rate dependency, which justified the use of the Rabinowitch correction. The power law index was 0.66. From the shift factor the activation energy of the shear viscosity was calculated to be 11.2 kcal/mol, which was near to the value found in the literature.¹⁹ With this flow activation energy and the estimated 9.7°C temperature increase in an adiabatic flow calculated previously the maximum decrease of shear viscosity by heating was estimated to be about 30%. However, the corresponding increase of shear viscosity due to pressure effect was about 4.7 times. This outweighed the thermal effect and produced an upward curvature as die length increased.

Extensional viscosities were calculated using eqs. (5) and (6) using true wall shear stress τ_{tw} in place of τ_w . The results of extensional viscosity are shown in Figure 6. The results were also shifted to 190°C by time-temperature superposition using the same shift factors determined from shear viscosity. A reasonable master curve was formed from the data of the three temperatures. Without this shift the extensional viscosity at higher temperature was lower. The dependency of extensional viscosity with respect to extensional strain rate showed a decreasing trend when strain rate increased. It was also a power law type with a similar power law index compared to the melt viscosity. At the higher strain rate, which

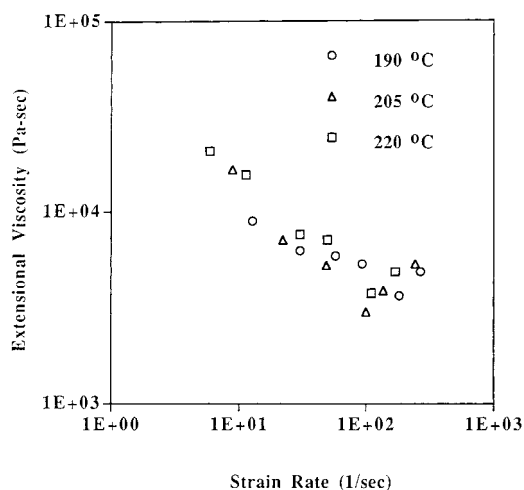


Figure 6 Extensional viscosity vs. extensional strain rate of polypropylene. Symbols: (○) 190°C; (△) 205°C; (□) 220°C. Data were shifted to 190°C using the same shift factors as Figure 5.

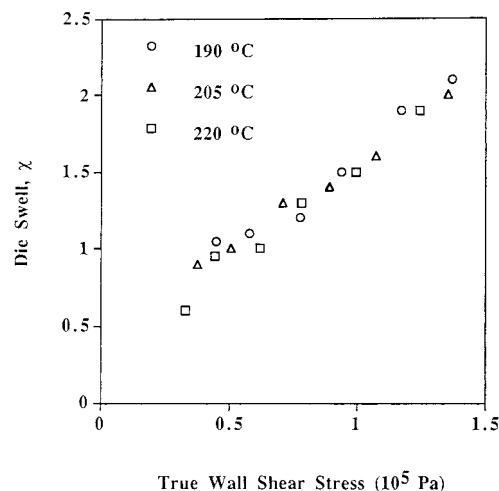


Figure 7 Die swell ratio of polypropylene with 10 mm die. Symbols: (○) 190°C; (△) 205°C; (□) 220°C.

corresponded to the higher shear rate in the capillary measurement, an upward deviation was observed. This was due to the melt fracture that produced additional pressure loss and was included in the end effect as well as extensional viscosity calculation.

The extensional viscosity of a linear polymer is three times the shear viscosity in the Newtonian region.^{4,8} This was demonstrated by Hingman and Marczinke⁸ for polypropylene using data of uniaxial elongational flow experiments and cone and plate rheometer measurements. In their results the Newtonian region was reached at a deformation rate below 0.001 s^{-1} . These authors also showed that the extensional viscosity results of uniaxial elongational flow and Cogswell's method matched very well in the strain rate from 0.1 to 1 s^{-1} . In the present study the lowest shear rate was 100 s^{-1} and the strain rate was 10 s^{-1} . These were far above 0.001 s^{-1} . Therefore, the results were in the power law region. In this region the ratio of extensional viscosity was about 10 times shear viscosity. This ratio was comparable to the results of Binding et al.¹⁴ in the same shear region.

Die swell was calculated by taking the ratio of diameter of the solid extrudate to the capillary diameter. This method has a tendency to underestimate the value because of the shrinkage due to cooling and crystallization. But it still provided some results for comparison. Die swell data of the 10-mm die are plotted vs. true wall shear stress in Figure 7. Similar data for the 20- and 30-mm dies are plotted in Figures 8 and 9, respectively. It can

be seen that the die swell increased when the shear stress increased. In each figure the results of the three temperatures fall on a master curve with an increasing trend. Grassley et al.²⁰ showed that for polystyrene a similar plot of die swell ratio vs. wall shear stress also fell on a master curve. Tzoganakis et al.⁹ showed similar results for polypropylene. More recently, Brando et al.²¹ showed that die swell ratios of two grades of polypropylene could be summarized as functions of wall shear stresses.

At low shear stress the die swell ratios were less than unity, indicating that diameters of the extrudates were smaller than the diameters of the dies. For Newtonian flow, theoretical analysis gave a die swell ratio of 1.12 at Reynolds numbers below 16.²⁰ The experimental results in this study could happen because of several reasons. One reason is the drawdown of the extrudate during extrusion by the weight of the extrudates. Another reason is the rapid cooling of the polymers, which prevent the complete recovery of strain and shrinkage of the polymers after cooling from the melt temperature. This was evident because the highest shrinkage occurred at the highest melt temperature. It was particularly noticeable in Figure 9. At high shear rate the die swell ratio of longer dies was lower. This is because a longer die provided longer time for relaxation, and the recovery of polymers from stretch was not so significant for longer dies. When the ratio L/R is sufficiently large the die swell will reach an asymptotic value. The value of such L/R depends on the type of polymers used.^{21,22}

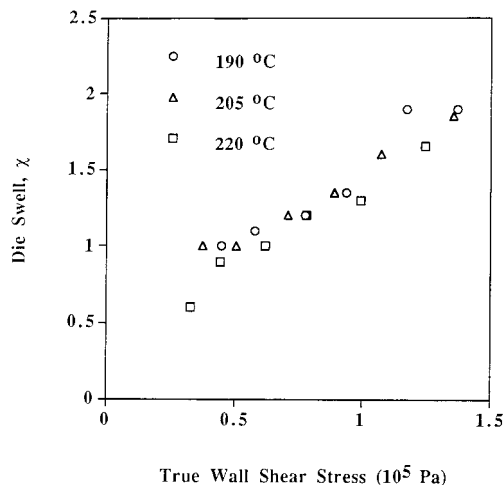


Figure 8 Die swell ratio of polypropylene with a 20-mm die. Symbols: (○) 190°C; (△) 205°C; (□) 220°C.

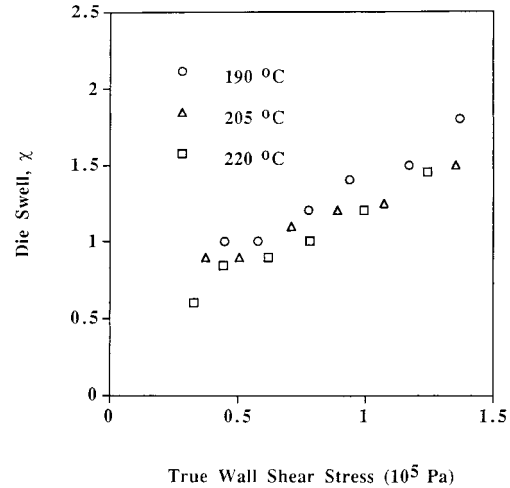


Figure 9 Die swell ratio of polypropylene with 30-mm die. Symbols: (○) 190°C; (△) 205°C; (□) 220°C.

CONCLUSIONS

Pressure effects on melt viscosities and the end effect were considered in the capillary flow and a new equation relating pressure and die length was derived. The equation was applied to a polypropylene resin using three capillary dies. The extrudate showed a visible melt fracture at the highest shear rate, which was also confirmed in the plot of end effect vs. true wall shear stress. Melt viscosity and extensional viscosity were calculated as functions of shear rate and strain rate, respectively. Both properties correlated well after time-temperature superposition shift and showed power law behaviors. Extensional viscosity showed an upward trend when melt fracture occurred. Die swell ratios increased when true wall shear stress increased but decreased when capillary length increased.

The authors would like to express their special thanks to Dr. R. D. Deanin of the Department of Plastics Engineering at the University of Massachusetts Lowell for his invaluable help and useful discussion.

REFERENCES

1. Middleman, S. *Fundamentals of Polymer Processing*; McGraw-Hill: New York, 1977.
2. Rammurthy, A. V. *J Rheol* 1986, 30, 337.
3. Denn, M. M. *Annu Rev Fluid Mech* 1990, 22, 13.
4. Gupta, R. K. *Polymer and Composites Rheology*; Marcel Dekker: New York, 2000, 2nd ed.
5. Bagley, E. B. *J Appl Phys* 1957, 28, 624.

6. Rabinowitsch, B. Z. *Phys Chem* 1929, A145, 1.
7. Cogswell, F. N. *Polym Eng Sci* 1972, 12, 64.
8. Hingmann, R.; Marcinke, B. L. *J Rheol* 1994, 38, 573.
9. Tzoganakis, C.; Vlachopoulos, J.; Hamielec, D. E.; Shinozaki, D. M. *Polym Eng Sci* 1989, 29, 390.
10. Kamal, M. R.; Nyun, H. *Polym Eng Sci* 1980, 20, 109.
11. Huang, J. C.; Shen, H. F. *Adv Polym Technol* 1989, 9, 211.
12. Huang, J. C.; Liu, H.; Liu, Y. *Polym Plast Tech Eng* 2001, 40, 79.
13. Kazatchkov, I. B.; Hatzikiakos, S. G.; Stewart, C. W. *Polym Eng Sci* 1995, 35, 1864.
14. Binding, D. M.; Couch, M. A.; Walters, K. J. *Non-Newtonian Fluid Mech* 1998, 79, 137.
15. Vlachopoulos, J.; Alam, M. *Polym Eng Sci* 1972, 12, 184.
16. Ui, J.; Ishimaru, Y.; Murakami, H.; Fukushima, N.; Mori, Y. *SPE Trans* 1964, 295.
17. Baik, J. J.; Tzoganakis, C. *Polym Eng Sci* 1998, 38, 274.
18. Ferry, J. D. *Viscoelastic Properties of Polymers*; Wiley: New York, 1980, 3rd ed.
19. van Krevelen, D. W. *Properties of Polymers—Their Estimation and Correlation with Chemical Structure*; Elsevier: Amsterdam, 1976, 2nd ed.
20. Graessley, W. W.; Glasscock, S. D.; Crawley, R. L. *Trans Soc Rheol* 1970, 14, 519.
21. Brandao, J.; Spieth, E.; Lekakon, C.; Polibrasil, S. A. *Polym Sci Eng* 1996, 36, 49.
22. Tanner, R. L. *J Polym Sci A2* 1970, 8, 2067.